

Because of the smaller range and quantity of 'coesite' data, it is not possible to determine as many parameters of the equation of state as were determined for the stishovite data. Because the data extend to only about 15% volume compression, it is not necessary to use the full fourth-order version of (3), and so the  $\epsilon^3$  term is here assumed to be zero. Because there is not a large range in the initial porosities of the Hugoniot data, the volume dependence of  $\gamma$ , and hence  $(\partial K/\partial T)_P$ , cannot be well determined. Conversely, the value of  $(\partial K/\partial T)_P$  does not strongly affect the equation of state in this range. A value of  $-0.05$  kb/°K was therefore assumed. This value of  $(\partial K/\partial T)_P$  gives values of  $\delta_T$  in the range 5–10, a range that seems reasonable on the basis of a few other examples, including stishovite [e.g., *Anderson et al.*, 1968; *Roberts and Ruppini*, 1971]. The values of  $V_0$  and  $\alpha$  were taken from Table 2, and  $C_0$  was calculated from the Debye model.

It can be seen from Figure 1 that the  $\rho_0' = 1.35$  g/cm<sup>3</sup> Hugoniot data are considerably scattered and that they do not trend toward the coesite density of 2.91 g/cm<sup>3</sup>, perhaps because there has been a partial conversion to the stishovite phase. When they are compared to the  $\rho_0' = 1.15$  g/cm<sup>3</sup> Hugoniot data, the lower three points in particular are seen to deviate toward higher densities. Two cases were therefore treated, one including these three points, the other excluding them.

Initially both  $K_0$  and  $K_0'$  were determined by the Hugoniot and static-compression data. The results are given as cases 1 and 2 in Table 6, case 1 excluding the three doubtful Hugoniot points and case 2 including them. The standard errors used to weight the compression data are given in Table 5. Case 1 is illustrated in Figure 1, case 2 in Figure 6. The bulk moduli in these two cases are significantly above the value of 0.97 Mb measured ultrasonically by Mizutani et al. (H. Mizutani, private communication, 1972), and so a third case was run with  $K_0$  fixed at this value and only  $K_0'$  determined by the compression data (Table 6 and Figure 6). It can be seen (Figure 6) that case 3 does not fit the static-compression data of *Bassett and Barnett* [1970] very well, and it falls below most of the corresponding Hugoniot data.

The scatter in the Hugoniot data and the uncertainty in their interpretation are such that

TABLE 5. Standard Errors Assumed for the 'Coesite' Compression Data

Data	Error, Mb
S11	0.20
S12	0.10
S13	0.10
X3	0.02

they cannot definitely be said to be discordant with case 3, but the discrepancy between case 3 and the static-compression data seems to be significant. Because of this discrepancy, the equation of state of coesite must remain somewhat uncertain at this stage.

#### SiO<sub>2</sub> PHASE EQUILIBRIA

By using the equations of state just given, the Gibbs free energies of 'coesite' and stishovite can now be calculated, and the 'coesite'-stishovite transition pressure can be calculated as a function of temperature by using the condition that the Gibbs free energies of the two phases are equal at the phase transition.

For detailed comparison the Hugoniot temperatures, which were calculated approximately by *Trunin et al.* [1971b], have been calculated according to the method described earlier. The results are plotted against Hugoniot pressure (Figures 7 and 8). It is notable that the 5.5-Mb point is over 40,000°K and that the  $\rho_0' = 1.77$  point at 2.3 Mb is over 30,000°K. The temperatures are changed by only a few per cent by using the different equations of state given in the previous sections. A greater uncertainty in the points is due to the scatter in Hugoniot pressures, but this scatter would only cause

TABLE 6. 'Coesite' Parameters for Various Cases

Case	$K_0$ , Mb	$K_0'$	$(\partial K_0/\partial T)_P^*$	$\gamma$	$\frac{d \ln \gamma}{d \ln V}$	$\delta_T$
1	1.27	5.6	-0.05	0.43	-0.04	4.9
2	1.36	4.1	-0.05	0.46	1.2	4.6
3	0.97†	7.3	-0.05	0.33	-0.15	6.4

\*Assumed values (see text).

†Fixed value from Table 2.



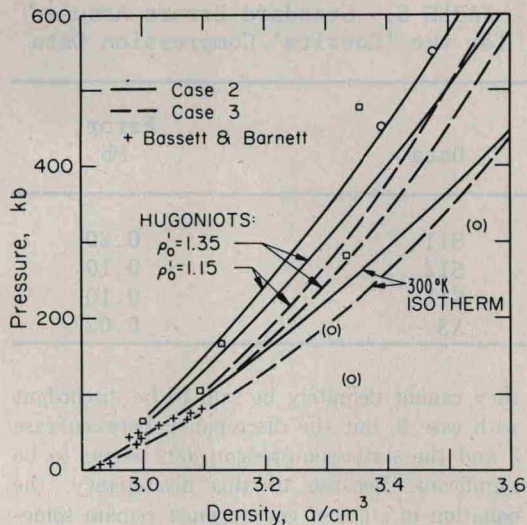


Fig. 6. Hugoniot data of 'coesite' and calculated Hugoniot and 300°K isotherms from cases 2 and 3 (Table 6). Symbols are those used in Figures 1 and 5.

the points to move along the Hugoniot locus, which in a  $P$ - $T$  plot is approximately radial from the initial point.

The boundary between the 'coesite' and stishovite fields (Figure 8) is closely defined by the  $\rho_0' = 1.77$  and  $\rho_0' = 1.55$  g/cm<sup>3</sup> Hugoniot points, both of which show signs involving a mixture of the two phases, as was discussed earlier.

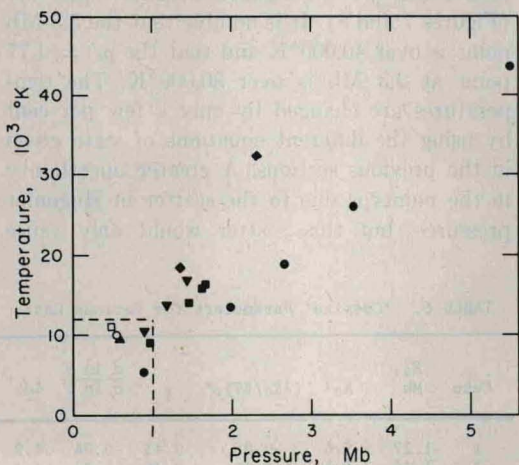


Fig. 7. Calculated Hugoniot temperatures of stishovite and 'coesite' versus Hugoniot pressure. Box is enlarged in Figure 8. Symbols are those used in Figure 1.

The Gibbs free energy is defined by

$$G = H - TS = U + PV - TS \quad (14)$$

where  $H$  is the enthalpy and  $S$  is the entropy. Here  $G$  has the property [e.g., Slater, 1939]

$$(\partial G/\partial P)_T = V \quad (15)$$

We wish to evaluate  $G$  at the state  $(P, V, T)$ , starting from the state  $(0, V_0, T_0)$ . (Atmospheric pressure can be ignored here.) This evaluation will be done via the state  $(P_0, V_0, T)$ , where  $P_0(T) = P(V_0, T)$  (i.e., by first raising the temperature at constant volume and then compressing isothermally). From (14)

$$\begin{aligned} G(V_0, T) &= G(V_0, T_0) \\ &+ [U(V_0, T) - U(V_0, T_0)] + P_0(T)V_0 \\ &- [TS(V_0, T) - T_0S(V_0, T_0)] \end{aligned} \quad (16)$$

and from (15), upon integration,

$$G(V, T) = G(V_0, T) + \int_{P_0(T)}^{P(T)} V(P', T) dP' \quad (17)$$

When the difference between the Gibbs free energies of stishovite and coesite at the state  $(V_0, T_0)$  are denoted by  $\Delta G_0$  (i.e.,

$$\Delta G_0 = G^s(V_0^s, T_0) - G^c(V_0^c, T_0)$$

where superscripts  $s$  and  $c$  denote stishovite and

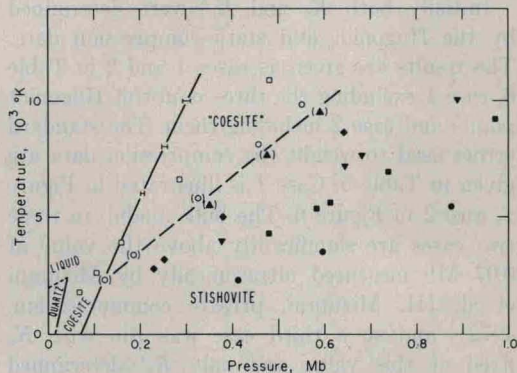


Fig. 8. Calculated Hugoniot temperatures of stishovite and 'coesite' versus Hugoniot pressure compared with observed and calculated (solid and short-dashed) phase lines. Long-dashed line separates stishovite and 'coesite' fields. Error bars represent variations due to the use of alternative equations of state given in previous sections. Symbols are those used in Figure 1.